Simulation-based Assessment of the Impact of Contrast Medium on CT-based Attenuation Correction in PET

Mohamad Reza Ay, *Member, IEEE, and* Habib Zaidi, *Senior Member, IEEE*

***Abstract*— Although diagnostic quality CT relies on the administration of contrast agents to allow improved lesion detectability, the misclassification of contrast medium as high density bone during CT-based attenuation correction (CTAC) procedure is known to overestimate the attenuation coefficients, thus biasing activity concentration estimates of PET data. In this study, the influence of contrast medium on CTAC was investigated through Monte Carlo (MC) simulations and experimental phantom studies. Our recently developed MC x-ray CT simulator and the *Eidolon* 3D PET MC simulator were used to generate realigned PET/CT data sets. The influence of contrast medium was studied by simulation of a cylindrical phantom containing different concentrations of contrast medium. Moreover, an experimental study using an anthropomorphic striatal phantom was conducted for quantitative evaluation of errors arising from the presence of contrast medium by calculating the apparent recovery coefficient (ARC). The ARC was 190.7% for a cylindrical volume of interest located in the main chamber of the striatal phantom containing contrast medium corresponding to 2000 Hounsfield units, whereas the ARC was overestimated by less than 5% for the main chamber and 2% for the left/right putamen and caudate nucleus compared to the absence of contrast medium. It was concluded that the contrast-enhanced CT images may create considerable artifacts during CTAC in regions containing high concentrations of contrast medium.**

I. Introduction

Combined PET/CT systems offer significant advantages over stand alone PET including decreased overall scanning time and increased accuracy in tumor localization and detectability. However, the use of CT images for attenuation correction of PET data in presence of contrast medium is known to generate visible artifacts in the resulting PET images in some cases [1]. The misclassification of contrast medium with high density bone in commonly used CT-based attenuation correction (CTAC) algorithms is known to overestimate the attenuation map (μmap), thus resulting in overestimation of activity concentration in PET images. The limited number of publications assessing the impact of contrast medium using phantom studies where the ground truth is known and their limitations in terms of the complexity of simulated shapes, usually restricted to simple uniform cylindrical phantoms, spurred the research presented in this paper where a more realistic anthropomorphic striatal phantom and accurate modeling of contrast medium through Monte Carlo simulations combined with geometric transfer matrix (GTM)-based partial volume correction for accurate quantitative analysis were used. The aim of this study was to investigate the impact of contrast medium in CT images on the accuracy of CTAC at different levels, including raw data acquisition, generated attenuation maps, attenuation correction factors (ACFs) and reconstructed PET emission images, using dedicated x-ray CT and 3D PET Monte Carlo simulations combined with experimental phantom studies.

This work was supported by the Swiss National Science Foundation under grant SNSF 3152A0-102143.

Mohammad Reza Ay was with the Division of Nuclear Medicine, Geneva University Hospital, CH-1211 Geneva, Switzerland. He is now with the Department of Medical Physics, Tehran University of Medical Sciences, Tehran, Iran (e-mail: mohammadreza_ay@tums.ac.ir).

Habib Zaidi is with the Division of Nuclear Medicine, Geneva University Hospital, CH-1211 Geneva, Switzerland (e-mail: habib.zaidi@hcuge.ch)

II. Materials and Methods

A. Monte Carlo Simulations

Our recently developed MCNP4C-based Monte Carlo x-ray CT simulator [2] was used for modeling of LightSpeed four-slice CT scanner (GE Healthcare Technologies, Waukesha, WI) and the *Eidolon* dedicated 3D PET Monte Carlo simulator [3] was used to generate realigned PET/CT data sets corresponding to the geometry of the ECAT ART PET scanner (CTI/Siemens, Knoxville, TN). Experimental and/or clinical validation of the PET and CT simulators has been described in the above mentioned references.

B. Experimental Phantom Measurements

Given that a combined PET/CT scanner was not available to us during the actual study design, our investigation relied on the use of PET and CT data acquired on separate PET and CT scanners. One of the motivations behind the choice of brain imaging is that automated multimodality coregistration algorithms work relatively well (in contrary to whole-body imaging) and can be applied most successfully to neurological studies, where the skull provides a rigid structure that maintains the geometrical relationship of structures within the brain.

A polyethylene cylindrical phantom (250±0.5 mm diameter) containing 16 cylindrical holes (20±0.5 mm diameter) was

constructed. Fourteen syringes were filled with a solution of K_2HPO_4 and water with concentrations varying between 50 mg/cm^3 and 900 mg/cm^3 to simulate cortical bone with different densities. The prepared syringes and two additional syringes containing water and air were inserted into the polyethylene phantom's holes. Thereafter, the phantom was scanned using the LightSpeed four-slice CT scanner to calculate the calibration curve for conversion from CT numbers to linear attenuation coefficients at 511 keV according to the method proposed by Bai *et al.* [4]. The XCOM photon cross section library [5] was used for calculation of the linear attenuation coefficients of the inserted solutions at 511 keV.

To investigate the effect of contrast medium on CTAC, experimental measurements of the anthropomorphic striatal phantom (Radiology Support Devices Inc., Long Beach, CA) were performed. This phantom consists of four small cavities that can be filled independently representing the left and right caudate and left and right putamen. In addition, there is a larger main chamber surrounding the four small cavities representing the rest of the brain. The main chamber itself is embedded in a bone like structure representing the skull. This arrangement provides properties similar to the human head suitable for mimicking PET studies of the presynaptic and postsynaptic dopaminergic system. For an activity concentration ratio of 1:8 between the main chamber and small cavities, 2.94 MBq of ^{18}F (in 0.9 ml, 0.9% NaCl) were diluted in distilled water. A total activity of 13.2 MBq ^{18}F diluted into 1.1 ml NaCl was filled into the main chamber. Subsequently, the main chamber was totally filled with distilled water. The fully 3D emission study lasted 25 minutes whereas the CT data of the same phantom were acquired using the Aquilion CT scanner (Toshiba Medical Systems Corporation, Tokyo, Japan) at 120 kV and 240 mA.

C. Attenuation Correction and Image Reconstruction

The computation of ACFs derived from CTAC involved down-sampling the CT image matrix to 128×128 followed by Gaussian smoothing using a 6 mm kernel to match the spatial resolution of the PET scanner used in this study. CT numbers (in HU) were then transformed to linear attenuation coefficients at 511 keV using the calculated bi-linear calibration curve. The created μmaps were forward projected to generate 47 ACF sinograms. The attenuation corrected projections were reconstructed using the 3DRP reprojection algorithm implemented within the ECAT 7.2.1 software (CTI Molecular Imaging Inc., Knoxville, TN) with a maximum acceptance angle corresponding to 17 rings and a span of 7. The default parameters used in clinical routine were applied (Ramp filter, cut-off frequency 0.35 cycles/pixel). The reconstructed images consist of 47 slices with 128×128 resolution and a voxel size set to 1.72×1.72×3.4 mm^3. Since the PET and CT data used in this study were acquired on separate PET and CT scanners, PET to CT image coregistration was performed using the commercial Hermes multi-modality fusion software (Nuclear Diagnostics AB, Stockholm, Sweden). In order to increase the accuracy of quantitative analysis of reconstructed PET images, correction for partial volume effect was performed using the popular geometric transfer matrix (GTM)-based method proposed by Rousset *et al.* [6] which allows to compute corrected estimates without *a priori* knowledge on any activity level.

D. Contrast Medium Modeling

The influence of contrast medium was studied by simulation of a cylindrical phantom containing different concentrations of contrast medium. Moreover, an experimental study using an anthropomorphic striatal phantom was conducted for quantitative evaluation of errors arising from the presence of contrast medium by calculating the apparent recovery coefficient (ARC) in presence of different artificially created concentrations of contrast medium in a cylindrical region in the main chamber of the striatal phantom. The ARC represents the apparent (observed or partial volume corrected) regional radioactivity concentration to true activity ratio. Two experiments were carried out to assess the impact of contrast medium on CTAC. Firstly, CT scans of a cylindrical water phantom (200 mm diameter) containing a centered cylinder (50 mm diameter) filled with different concentrations of iohexol were simulated. Iodine concentrations of 0.7 mg/cm^3, 3.5 mg/cm^3, 7 mg/cm^3 and 70 mg/cm^3 were considered for simulation of contrast medium solution (dilution of 1:500, 1:100, 1:50 and 1:5 of iohexol, respectively). Iohexol contrast medium was used as reference to validate simulated CT images by comparison with similar published experimentally measured CT numbers for the chosen concentrations. Thereafter, the reconstructed CT images were used for attenuation correction of the equivalently simulated PET data sets. In the second experiment, CT images of the anthropomorphic striatal phantom were modified by inserting a cylindrical region (20 mm diameter) in the main chamber to simulate the presence of contrast medium with various concentrations corresponding to CT numbers of 50, 100, 200, 500, 1,000, 1,500 and 2,000 HU. Subsequently, the resultant CTAC μmap was used for attenuation correction of emission data.

III. Results

Figure 1 shows the calculated bi-linear calibration curves for both CT scanners used in this study at 120 kVp tube voltage. The XCOM photon cross sections database was used for calculation of the corresponding linear attenuation coefficients of the inserted solutions at 511 keV.

As an illustration of the effect of the presence of positive contrast medium in a circular region located at the center of a water-filled cylinder, Fig 2 shows Monte Carlo generated attenuation profiles and scatter to primary ratios (SPR) using different concentrations of contrast medium for both x-ray

spectra and 511 keV. The attenuation profiles illustrate the significant difference in photons attenuation by contrast media between the two energies. The SPR is a good indicator of the scatter component's magnitude in the acquired data. The corresponding central profiles of the derived μmaps from reconstructed images in both energies and for two extreme cases of Iodine concentration (maximum of 70 mg/cm^3 and minimum of 0.7 mg/cm^3) are also shown (Figs. 3) to illustrate the impact of using contrast media on generated μmaps.

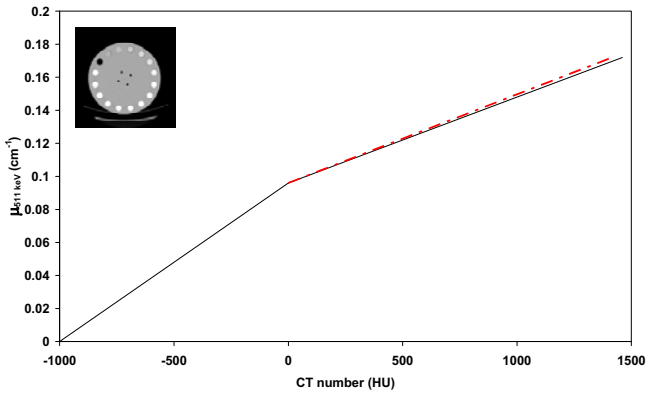

Fig. 1. Calculated bi-linear calibration curves for conversion of CT numbers (HU) at 120 kVp into linear attenuation coefficients at 511 keV for both Aquilion (solid line) and LightSpeed (dashed line) CT scanners. The in-house designed polyethylene cylindrical phantom containing 16 cylindrical holes is shown in the upper left corner.

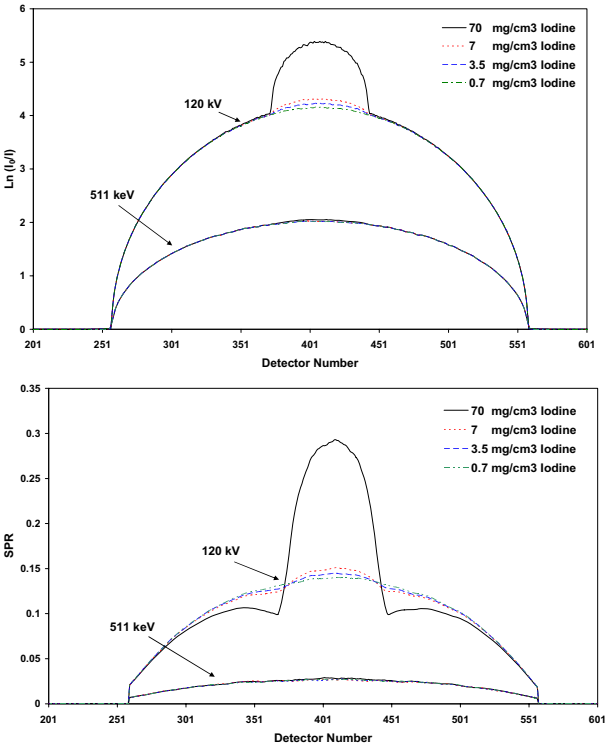

Fig. 2. Monte Carlo study of the impact of contrast medium in a cylindrical water phantom (200 mm diameter) containing a centered cylinder (50 mm diameter) having different concentrations of iohexol for both CT and monoenergetic 511 keV energies showing: (top) Attenuation profiles; (bottom) Scatter to primary ratios.

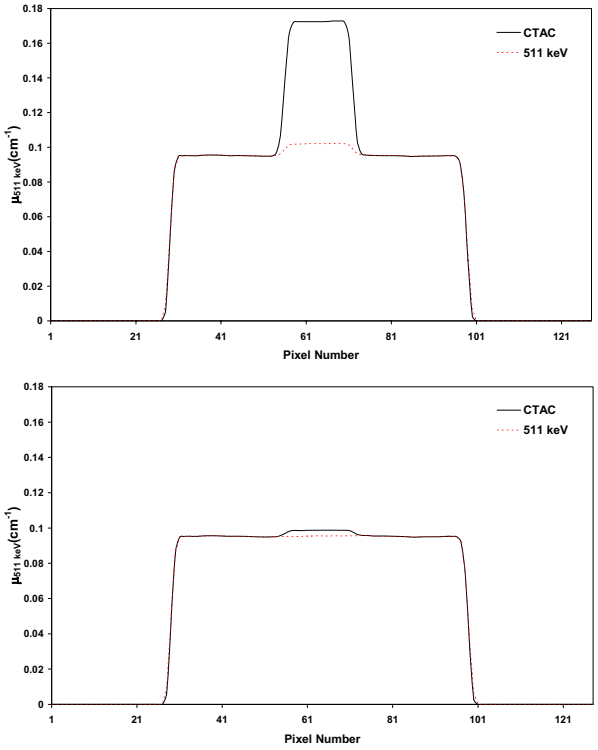

Fig. 3. Monte Carlo study of the impact of contrast medium in a cylindrical water phantom containing centered cylinder having different concentrations of iohexol for both CT and monoenergetic 511 keV energies showing: (top) central profiles through attenuation maps for maximum concentration (70 mg/cm^3 Iodine) of contrast medium; (bottom) for minimum concentration (0.7 mg/cm^3 Iodine) of contrast medium.

The computed ACF sinograms were used for attenuation correction of simulated emission data. Fig. 4 illustrates the μmaps and corresponding reconstructed emission images corrected for attenuation using CTAC for different concentrations of Iodine.

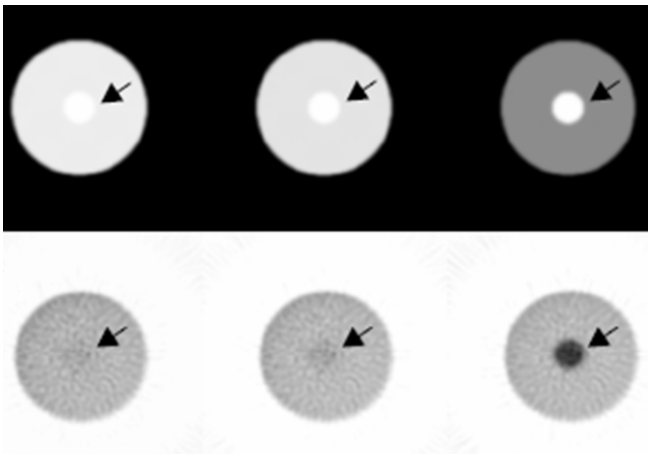

Fig. 4. Representative slice of calculated attenuation maps and reconstructed emission images for different concentrations of contrast medium: (top) MC simulated μmaps for different concentrations of contrast medium,

from left to right 3.5, 7 and 70 mg/cm^3 iodine; (bottom) corresponding reconstructed PET emission data following CTAC.

The simulated attenuation profiles for both energies are further validated by comparing average CT numbers in the contrast region of the uniform cylindrical phantom with published experimentally measured values [7] and theoretical linear attenuation coefficients computed using the XCOM photon cross section library [5] at 511 keV (Table I).

TABLE I

COMPARISON OF AVERAGE SIMULATED AND PUBLISHED MEASURED CT NUMBERS AND SIMULATED AND THEORETICAL LINEAR ATTENUATION COEFFICIENTS IN BOTH CT (120 KV_p) AND 511-KEV MONOENERGETIC ENERGIES

Concentration of Iodine in solution	Measured CT number (HU) [7]	Simulated CT number (HU)	Theoretical $\mu_{511\ keV}$ (cm^{-1}) XCOM [5]	Simulated $\mu_{511\ keV}$ (cm^{-1}) MCNP4C
70 mg/cm^3	1445.3	1434.8	0.1026	0.1028
7 mg/cm^3	205.7	193.2	0.0965	0.9677
3.5 mg/cm^3	128.2	118.2	0.0962	0.0964
0.7 mg/cm^3	65.3	50.2	0.0959	0.0961
0 mg/cm^3	9.7	1.3	0.0958	0.0960

Fig. 5 shows μmaps resulting from the conversion of CT images of the RSD striatal phantom modified by inserting positive contrast medium in a cylindrical region (20 mm diameter) in the main chamber containing different concentrations of contrast medium. The corresponding PET emission data corrected for attenuation using the generated μmaps and reconstructed using the 3DRP reprojection algorithm are also shown. Fig. 6 illustrates the calculated activity concentration in different regions of the striatal phantom after partial volume correction. A more rigorous quantitative measure of the effect of contrast medium is also given in Table II, which shows the apparent recovery coefficients (ARCs) calculated for six different regions in the RSD striatal phantom after partial volume correction using the GTM-based method [6].

IV. DISCUSSION

PET/CT now has emerged as an important and cost-effective method of performing anatomical-functional correlations in a way that improves patient management. However, in addition to a much higher absorbed dose to the patient, there are many physical and physiological factors that hamper the accurate registration of both imaging modalities and the accurate quantitative analysis of PET data following CTAC, the presence of oral and intravenous contrast medium being one of them. The impact of the presence of positive contrast agents on the accuracy of CTAC was investigated in both the effective energy of the x-ray tube and mono-energetic 511 keV photons at the level of CT images, resulting μmaps, ACF sinograms, and finally the reconstructed emission images. The first objective was reached through Monte Carlo simulations to confirm that the behaviour of contrast medium with respect to photon absorption and scattering is completely different between CT and 511 keV energies. The remaining experiments aimed to study the impact of contrast medium quantitatively by calculating ARCs in different regions of the RSD striatal phantom corrected for attenuation using CTAC for different concentrations of contrast medium (Table II).

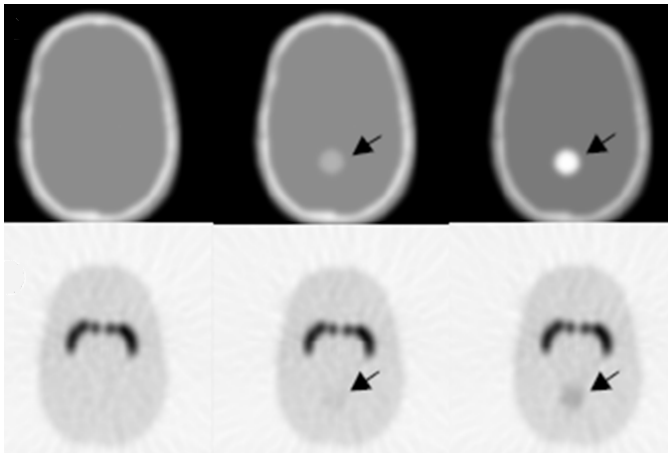

Fig. 5. Representative slice of calculated attenuation maps and reconstructed emission images for different concentrations of contrast medium: (top) calculated μmaps following modification of the striatal phantom by insertion of a cylindrical area containing different concentrations of contrast medium, from left to right 0, 500 and 2000 HU; (bottom) reconstructed PET emission images of the same phantom.

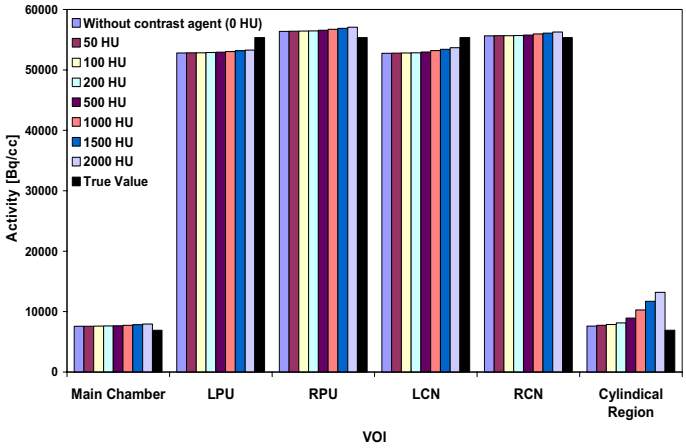

Fig. 6. Calculated activity concentrations in different volumes of interest (VOIs) after partial volume effect correction in the modified RSD anthropomorphic striatal phantom following insertion of a cylindrical VOI containing contrast medium in CT images.

The difference between attenuation profiles for various concentrations of contrast medium at CT energy (120 kVp) and 511 keV is due to the difference between the photon interaction cross sections at these energies. The difference between attenuation profiles calculated at 511 keV for various concentrations of contrast medium is insignificant whereas there is significant difference between attenuation profiles

calculated at CT energy. The high value of SPR in the region containing contrast medium at CT energy (Fig. 2) is due to the high absorption of primary photons by the contrast medium since the scatter distribution is approximately uniform. The curvature of SPR at 511 keV is due to the variable transmission probability of primary photons, which depends on the angle-dependent pathlength of attenuating media. It should be noted that the presence of contrast medium in the central area of the phantom has negligible impact on the SPR profile at 511 keV while its effect is significant at CT energy. The difference between μmaps and ACF sinograms generated using simulated CT images at CT energy and 511 keV (Fig. 3) for minimum (0.7 mg/cm^3 Iodine) and maximum (70 mg/cm^3 Iodine) concentrations of contrast medium is a nice illustration of extreme imaging conditions and the propagation of errors in attenuation correction factors to the emission data during attenuation correction (Fig. 4). The overestimation of activity concentration in the central area of PET images corrected using μmaps derived at CT energies is due to overestimation of ACFs in the related region whereas the effect of contrast medium at 511 keV is negligible, even with the highest concentration of Iodine (70 mg/cm^3). The same observations were made using the RSD striatal phantom's data corrected for attenuation using CTAC for different concentrations of contrast medium in a cylindrical region (Fig. 5). The overestimation of activity in the cylindrical region is significant when using high concentration of contrast medium (90% for 2000 HU). However, it produces negligible effect on the far away located brain regions, namely less than 2% for the small regions (LPU, RPU, LCN and RCN) and 6% in the main chamber (Table II).

TABLE II

APPARENT RECOVERY COEFFICIENS (ARCS) FOR DIFFERENT VOIS AFTER PARTIAL VOLUME EFFECT CORRECTION IN MODIFIED RSD ANTHROPOMORPHIC STRIATAL PHANTOM BY INSERTING A CYLINDRICAL VOI CONTAINING CONTRAST MEDIUM IN CT IMAGES

Volume of interest (VOI)	Vol. (cm^3)	CT number in the cylindrical VoI 0	50	100	200	500	1000	1500	2000
Main chamber	1290	110	110	110	110	111	112	113	115
Left putamen (LPU)	6	95	95	95	95	96	96	96	96
Right putamen (RPU)	6	102	102	102	102	102	102	103	103
Left nucleus caudate (LCN)	4.9	95	95	95	95	96	96	96	97
Right nucleus caudate (RCN)	4.9	100	100	101	101	101	101	101	102
Contrast medium region	79.3	110	112	114	117	129	148	169	191

V. CONCLUSION

The impact of contrast medium on the accuracy of CT-based attenuation correction in PET was studied using Monte Carlo simulations combined with experimental phantom studies. It was concluded that contrast-enhanced CT images may create visible artefacts in regions containing high concentrations of contrast medium [9]. This study reports results from a limited set of computer simulation of realistic PET and CT systems combined with experimental measurements using validated techniques. Further research using experimentally measured dynamic whole-body anthropomorphic phantoms on operational systems installed recently in our department (Biograph16 and Biograph64, Siemens Medical Solutions) with a broader range of contrast medium concentrations, as well as more realistic geometries and sizes of the opacified structures representative of those imaged in clinical settings is guaranteed.

REFERENCES

[1] H. Zaidi and B. H. Hasegawa, "Determination of the attenuation map in emission tomography," *J Nucl Med*, vol. 44, pp. 291-315, 2003.

[2] M. R. Ay and H. Zaidi, "Development and validation of MCNP4C-based Monte Carlo simulator for fan- and cone-beam x-ray CT," *Phys. Med. Biol.*, vol. 50, pp. 4863-4885, 2005.

[3] H. Zaidi, A. H. Scheurer, and C. Morel, "An object-oriented Monte Carlo simulator for 3D cylindrical positron tomographs," *Comput. Methods Programs Biomed.*, vol. 58, pp. 133-145, 1999.

[4] C. Bai, L. Shao, A. J. Da Silva, and Z. Zhao, "A generalized model for the conversion from CT numbers to linear attenuation coefficients," *IEEE Trans Nucl Sci*, vol. 50, pp. 1510-1515, 2003.

[5] Berger MJ, Hubbell JH, Seltzer SM, Chang J, Coursey JS, Sukumar R*, et al.* XCOM: photon cross sections database. NBSIR 87-3597. 1998. Available at *http://physics.nist.gov/PhysRefData/Xcom/Text/XCOM.html*

[6] O. G. Rousset, Y. Ma, and A. C. Evans, "Correction for partial volume effects in PET: principle and validation," *J Nucl Med*, vol. 39, pp. 904-911, 1998.

[7] Y. Nakamoto, B. B. Chin, D. L. Kraitchman, L. P. Lawler, L. T. Marshall, and R. L. Wahl, "Effects of nonionic intravenous contrast agents in PET/CT imaging: phantom and canine studies," *Radiology*, vol. 227, pp. 817-824, 2003.

[8] D. W. Townsend, J. P. J. Carney, J. T. Yap, and N. C. Hall, "PET/CT today and tomorrow," *J Nucl Med*, vol. 45, pp. 4s-14s, 2004.

[9] M. R. Ay and H. Zaidi, "Assessment of errors caused by x-ray scatter and use of contrast medium when using CT-based attenuation correction in PET," *Eur J Nucl Med Mol Imaging*, vol. 33, 2006 *in press*